Enhanced PMU-based Line Parameters Estimation and Compensation of Systematic Measurement Errors in Power Grids Considering Multiple Operating Conditions

Carlo Sitzia, *Student Member, IEEE*, Carlo Muscas, *Senior Member, IEEE*, Paolo Attilio Pegoraro, *Senior Member, IEEE*, Antonio Vincenzo Solinas, *Graduate Student Member, IEEE*, Sara Sulis, *Senior Member, IEEE*

***Abstract*—Several monitoring, protection, and control applications designed for modern power grids are based on detailed grid models and thus require an accurate knowledge of line parameters. A synchronized monitoring infrastructure based on Phasor Measurement Units (PMUs) may be of great support to the task of line parameters estimation, but the accuracy of the estimated parameters may be largely affected by the uncertainty of all the elements of the PMU-based measurement chain. Thus, an accurate parameters estimation must appropriately consider the metrological behavior of all these elements, and in particular that of instrument transformers. To address this challenge, the paper proposes an enhanced multi-branch method for accurate estimation of the line parameters and of the systematic measurement errors introduced by the instrument transformers when measurements for multiple operating conditions are considered. Indeed, multiple operating conditions are dealt with properly, thanks to an in-depth analysis of the problem modeling within the framework of Tikhonov regularization. The validity of the proposed approach is confirmed by the results obtained on the IEEE 14 bus test system.**

***Index Terms*—phasor measurement units, power transmission lines, instrument transformers, voltage measurement, current measurement, power grids.**

I. Introduction

The accurate knowledge of power grid line parameters is the basis of most advanced management, protection, and control applications. Nonetheless, the actual values of these parameters may largely differ from those stored in Energy Management System (EMS) database (see for example [1]), depending on a number of factors, like degradation due to age, modeling inaccuracies, etc., thus causing problems not only to the applications underlying the functioning of EMS, but also to the accuracy, reliability and economy of power dispatching control [2].

Phasor Measurement Units (PMUs), thanks to their ability to provide accurate absolute phase-angle measurements, represent an excellent tool to overcome some of the difficulties associated with traditional monitoring systems and have been widely installed in recent years by many Transmission System Operators (TSOs) all around the world. However, despite the high accuracy of PMUs, phasor measurements are affected by the uncertainty sources of the entire measurement chain. In particular, the effects of Instrument Transformers (ITs), i.e. Current Transformers (CTs) and Voltage Transformers (VTs), may significantly affect the accuracy of the measured phasors.

Therefore, for an effective use of network parameters values, it is necessary to apply an appropriate evaluation process, taking into account the uncertainties of the entire measurement infrastructure. Moreover, the estimation methods must be based on suitable models of such uncertainty sources, so that their effects can be properly taken into account and, if possible, minimized.

In the context of power grid protection, the law of propagation of uncertainty [3] is used, for example, in [4], where it is discussed how the fault location results are affected by the measurement uncertainty because the fault location algorithms typically need to use the available transmission line parameters. The problem of the uncertainty affecting transmission line parameters is also addressed in [5], where an analytical expression for the bounds of the transmission line parameters calculated directly from PMU measurements is derived. The same direct calculation is considered in [6] based on field tests. Systematic and random errors contributions of ITs and PMUs are considered, showing that the correlation between voltage and current measurements must be properly taken into account in the uncertainty propagation.

In the context of the line parameters estimation, several studies addressing different aspects of such estimation problem have been presented. Most of the papers consider only the uncertainty of the PMUs, see for example [7]. In [8], a PMU-based estimation of three-phase transmission line impedance parameters is proposed, where PMUs are considered to define the uncertainty but it is recognized that the accuracy of the VTs and CTs must be taken into account as well for the application of the proposal in actual grids. Other papers consider the presence of ITs, but, mostly, taking into account a given random uncertainty contribution, as in [9] and [10]. In [11], for example, the availability of pre-calibrated instrument transformers is assumed.

This research activity was partially supported by Fondazione di Sardegna under project "SISCO - ITC methodologies for the security of complex systems", CUP: F74I19001060007.

C. Sitzia, C. Muscas, P. A. Pegoraro, A. V. Solinas, and S. Sulis are with the Department of Electrical and Electronic Engineering of the University of Cagliari, Piazza d'Armi, 09123 Cagliari, Italy (email: [carlo.sitzia, carlo.muscas, paolo.pegoraro, v.solinas, sara.sulis]@unica.it).

In [12] the problem of simultaneous parameters estimation and compensation of systematic measurement errors is addressed neglecting the systematic phase errors of the voltages and the amplitude errors of the currents. In [13] the drawbacks that arise when overlooking bias errors are discussed and a new method is proposed by adding extra parameters in the regression model which account for the bias errors present in the non-calibrated ITs. Paper [14] presents a method for calibrating VTs online using synchrophasor measurements, finding the optimal locations where good quality measurements must be added in order to bring the calibration error of all the measurements below a predefined threshold. In [15], revenue transducers installed on a single bus in the system are exploited to propagate accuracy in the other nodes using network topological information. In [16] and [17], the problem of detection and correction of systematic errors in ITs along with line parameter estimation using unbiased PMU data is faced for a single branch, starting from bias error detection tests to identify systematic errors in ITs.

In this context, this paper addresses the problem of an effective simultaneous line parameters estimation and compensation of amplitude and phase-angle systematic errors of voltage and current synchrophasor measurements when multiple operating conditions are considered. No assumption is made about the presence of pre-calibrated devices. In particular, the paper improves the procedure proposed in [18], where the problem was addressed in the Weighted Least Squares (WLS) sense initially on a single branch and then on multiple branches considering few operating conditions. As underlined in [19], the line parameter estimation problem can be under-determined and it is necessary to exploit more snapshots of measurements in order to obtain an overdetermined system. Furthermore, in [20] the positive effect of adding measurements acquired in different time instants and corresponding to different operating conditions is highlighted, thus pointing to the importance of including multiple measurement sets in the estimation method. For these reasons, two or more operating conditions are used in the literature in the formulation of line parameters estimation problems, see for example [8], [14], [16] and [17]. In this context, PMUs allow acquiring several measurements per second, and thus it is important, for an estimation algorithm based on synchrophasor measurements, to deal with many available measurement sets.

This paper generalizes the estimation method by framing the WLS in [18] as a particular case of Tikhonov regularization and it thus provides a way to improve the estimation accuracy by tackling the management of multiple loading conditions in the estimation process. The main contributions of the paper are: it gives a framework to provide an optimization of the simultaneous estimation of line parameters and systematic errors in the presence of multiple operating conditions, it proposes a configuration criterion for the estimation problem and it introduces an enhanced multi-branch algorithm to leverage PMU capabilities in this context. The proposal is based on a detailed analysis of the estimation uncertainty.

II. Estimation Framework

A. Measurement Model and Network Constraints

A π-model as in Fig. 1 is considered for the generic branch (i, j) of a transmission network. In this paper, for the sake of a simpler introduction to the approach, an equivalent single-phase model of the three-phase system is considered as in [15]. A synchrophasor measurement unit (e.g. a PMU) is assumed to be available at each end of the line, thus allowing to measure two voltage synchrophasors (v_i and v_j for the start and end node, respectively) and two branch current synchrophasors (i_{ij} and i_{ji}). $z_{ij} = R_{ij} + jX_{ij}$ is the line impedance in the π-model, while $B_{sh,ij}$ represents the shunt susceptance, which is assumed equally divided into the two sides of the branch. The synchronized measurements can be time-aligned and thus represent a coordinated set of measurements referred to the same time instant t.

The line model defines a measurement model that links the set of measured values to the line parameters, which are not exactly known, and to the errors that affect every measured value. Each measured synchrophasor can be expressed as a function of reference values (indicated in the following equations by superscript ^{R}) and of measurement errors as follows:

$$\begin{aligned} v_h &= V_h e^{j\varphi_h} = V_h^r + jV_h^x \\ &= (1 + \xi_h^{sys} + \xi_h^{rnd}) V_h^R e^{j(\varphi_h^R + \alpha_h^{sys} + \alpha_h^{rnd})} \\ i_{ij} &= I_{ij} e^{j\theta_{ij}} = I_{ij}^r + jI_{ij}^x \\ &= (1 + \eta_{ij}^{sys} + \eta_{ij}^{rnd}) I_{ij}^R e^{j(\theta_{ij}^R + \psi_{ij}^{sys} + \psi_{ij}^{rnd})} \end{aligned} \tag{1}$$

where V_h and φ_h (with $h \in \{i, j\}$) are, respectively, the magnitude and phase-angle measurements of node h voltage, while I_{ij} and θ_{ij} are the measured magnitude and phase angle of the branch current flowing from node i towards node j. Measured current phasor i_{ji} (see Fig. 1) can be expressed in a similar way. Superscripts ^{r} and ^{x} are used for the real and imaginary parts of the corresponding phasors. The measurement errors can be either systematic or random (superscripts ^{sys} and ^{rnd}, respectively) and affect both magnitudes and phase angles of the phasors. Indeed, the parameters ξ_h and η_{ij} refer to the ratio errors, while α_h and ψ_{ij} are the phase displacement errors for the quantities in (1). The main difference between the two error typologies is that systematic errors do not vary across repeated measurements, while random errors give a different contribution for each observation. In this paper, as in [18], the idea underlying the estimation approach is that systematic errors in the measurement chain cannot be neglected and are

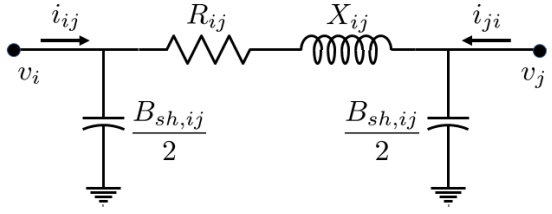

Fig. 1. π-model for a generic transmission network branch and its parameters.

thus considered unknown parameters to be estimated together with the line parameters.

The estimation algorithm is based on the definition of the constraints given by Kirchhoff's laws, which allow writing the relationships among line parameters, measured values and measurement errors. Since the Kirchhoff's laws are valid among actual values, equations in (1) need to be rewritten to explicit the reference values as functions of measurements and errors as in [18] (see (A.27) in Appendix A for details).

The complex equations derived from voltage drop constraint and from current balance constraint are:

$$\left(v_i^R - v_j^R\right) = z_{ij}\left(i_{ij}^R - j\frac{B_{sh,ij}}{2}v_i^R\right) \tag{2}$$

$$\left(i_{ij}^R + i_{ji}^R\right) = \frac{B_{sh,ij}}{2}\left(v_i^R + v_j^R\right) \tag{3}$$

where the line parameters can be expressed as a function of their values available in the TSO database (the only known values, here indicated with the superscript ^{0}) and their unknown deviations from those values:

$$\begin{aligned} z_{ij} &= R_{ij}^0\left(1+\gamma_{ij}\right) + jX_{ij}^0\left(1+\beta_{ij}\right) \\ B_{sh,ij} &= B_{sh,ij}^0\left(1+\rho_{ij}\right) \end{aligned} \tag{4}$$

where γ_{ij}, β_{ij} and ρ_{ij} are the relative deviations of actual values from nominal ones. These deviations are unknown and need to be estimated together with the other unknown quantities. This representation allows, under realistic assumptions, the linearization of measurement functions and allows introducing directly and homogeneously prior information as discussed in the following.

Replacing (4) and (A.27) in (2) and (3) and neglecting second order terms (see also [18]), four real-valued equations are obtained for each branch, whose derivation and detailed expressions are reported in Appendix A. From (A.28)-(A.31), it is clear that each constraint can be seen as an equivalent measurement that depends on the unknown systematic errors and deviations from nominal values of line parameters corresponding to the considered branch, and on the random measurement errors. Considering a single branch (i,j) and single measurement instant t (associated with the timetag of PMU measurements), the following system of equations can be defined [18]:

$$\begin{aligned} \mathbf{b}_{ij,t} &= \mathbf{H}_{ij,t}\begin{bmatrix} \xi_i^{sys} \\ \alpha_i^{sys} \\ \xi_j^{sys} \\ \alpha_j^{sys} \\ \eta_{ij}^{sys} \\ \psi_{ij}^{sys} \\ \eta_{ji}^{sys} \\ \psi_{ji}^{sys} \\ \gamma_{ij} \\ \beta_{ij} \\ \rho_{ij} \end{bmatrix} + \mathbf{E}_{ij,t}\begin{bmatrix} \xi_i^{rnd} \\ \alpha_i^{rnd} \\ \xi_j^{rnd} \\ \alpha_j^{rnd} \\ \eta_{ij}^{rnd} \\ \psi_{ij}^{rnd} \\ \eta_{ji}^{rnd} \\ \psi_{ji}^{rnd} \end{bmatrix} \\ &= \mathbf{H}_{ij,t}\mathbf{x}_{ij} + \mathbf{E}_{ij,t}\mathbf{e}_{ij,t} = \mathbf{H}_{ij,t}\mathbf{x}_{ij} + \boldsymbol{\epsilon}_{ij,t} \end{aligned} \tag{5}$$

where $\mathbf{b}_{ij,t}$ is the 4×1 vector of equivalent measurements at time t, $\mathbf{H}_{ij,t}$ is the measurement matrix expressing the linear measurement functions, while $\mathbf{E}_{ij,t}$ is the transformation matrix (Jacobian matrix) linking equivalent measurements random error vector $\boldsymbol{\epsilon}_{ij,t}$ to the measurement random errors in $\mathbf{e}_{ij,t}$. $\mathbf{x}_{ij}$ is the vector of unknowns.

Considering multiple branches altogether (a branch set Γ of cardinality l) at the same time, the problem can be defined considering all the voltage constraints (2) and the current equations (3) for all the branches $(i,j)\in\Gamma$. The unknowns are thus all the systematic errors of the measurements of voltage and current synchrophasors involved and all the line parameter deviations of the branches. The system in (5) grows to become a $4\times l$ set of equations with n unknowns (vector $\mathbf{x}_\Gamma$):

$$\mathbf{b}_{\Gamma,t} = \begin{bmatrix} \mathbf{b}_{i_1j_1,t} \\ \vdots \\ \mathbf{b}_{i_lj_l,t} \end{bmatrix} = \mathbf{H}_{\Gamma,t}\mathbf{x}_\Gamma + \mathbf{E}_{\Gamma,t}\mathbf{e}_{\Gamma,t} = \mathbf{H}_{ij,t}\mathbf{x}_\Gamma + \boldsymbol{\epsilon}_{\Gamma,t} \tag{6}$$

where subscript Γ indicates that unknowns, equations and measurements correspond to the given branch set. It is important to notice that the number of unknowns does not increase linearly with l since there are nodes and measurements shared among branches. This is indeed the reason why the solution of (6) is not the result of simple juxtaposition of individual branch problems like (5), but it allows improving the estimation.

The estimation problem defined by (6) is typically underdetermined. However, as mentioned in Section I, multiple time instants $t_1,\cdots,t_{N_t}$, that is multiple synchronized measurement sets, can be used and a new over-determined linear system can be defined as follows:

$$\begin{aligned} \mathbf{b}_\Gamma &= \begin{bmatrix} \mathbf{b}_{\Gamma,t_1} \\ \vdots \\ \mathbf{b}_{\Gamma,t_{N_t}} \end{bmatrix} = \begin{bmatrix} \mathbf{H}_{\Gamma,t_1} \\ \vdots \\ \mathbf{H}_{\Gamma,t_{N_t}} \end{bmatrix}\mathbf{x}_\Gamma + \begin{bmatrix} \mathbf{E}_{\Gamma,t_1} & & \\ & \ddots & \\ & & \mathbf{E}_{\Gamma,t_{N_t}} \end{bmatrix}\begin{bmatrix} \mathbf{e}_{\Gamma,t_1} \\ \vdots \\ \mathbf{e}_{\Gamma,t_{N_t}} \end{bmatrix} \\ &= \mathbf{H}_\Gamma\mathbf{x}_\Gamma + \mathbf{E}_\Gamma\mathbf{e}_\Gamma = \mathbf{H}_\Gamma\mathbf{x}_\Gamma + \boldsymbol{\epsilon}_\Gamma \end{aligned} \tag{7}$$

where it is important to highlight that the unknown vector $\mathbf{x}_\Gamma$ is common to all the time instants, whereas measurement matrix and random errors change with the timestamp. Due to the high reporting rate of PMUs (up to hundreds of measurements per second), different measurement sets can be considered either as the result of repeated observations of the same network load condition or as different snapshots of different network conditions. The former scenario will be referred to as repeated measurements in the following, while the latter will be indicated as "operating cases" or simply "cases" since it reflects variations in loads, generated powers, etc. Repeated measurements obtained within a small time interval (e.g. corresponding to 1 s or even less), can be averaged and used to define an averaged version of (7), with averaged matrices and vectors. This approach, which, besides minimizing the effects of random error contributions, allows reducing the system size, was proven to be valid in [21] and will be here adopted. Thus the system definition from here on is based on different cases and averaged repeated measurements for each case.

In addition to the information brought by different cases, prior information about the unknowns is also added [18]. This allows including the available prior knowledge, for instance, on IT precision class and on maximum parameters variability.

Considering the l branches and $N_\Gamma \leq 2l$ nodes in Γ, combining C different operating cases (while averaging repeated measurements) and adding prior information about unknowns, an over-determined and augmented linear system is obtained:

$$\begin{aligned}\mathbf{b}_{tot} &= \begin{bmatrix}\mathbf{b}_\Gamma \\ \mathbf{0}_{n\times 1}\end{bmatrix} = \begin{bmatrix}\mathbf{H}_\Gamma \\ \mathbf{I}_n\end{bmatrix}\mathbf{x}_\Gamma + \begin{bmatrix}\boldsymbol{\epsilon}_\Gamma \\ \mathbf{e}_{prior}\end{bmatrix} \\ &= \mathbf{H}_{tot}\mathbf{x}_\Gamma + \boldsymbol{\epsilon}_{tot}\end{aligned} \tag{8}$$

with $\mathbf{b}_\Gamma \in \mathbb{R}^m$, $\mathbf{H}_\Gamma \in \mathbb{R}^{m\times n}$, $\mathbf{H}_{tot} \in \mathbb{R}^{(m+n)\times n}$, $\mathbf{b}_{tot} \in \mathbb{R}^{m+n}$, where m is the number of involved Kirchhoff's constraints. $\mathbf{I}_n$ is the n-size identity matrix and $\mathbf{0}_{n\times 1}$ is the n-zeros vector. Then, $m = 4\times l\times C$ and the number of unknowns n includes both $2 \times N_\Gamma + 4 \times l$ systematic errors of the measurement chain and $3 \times l$ line parameter deviations (if γ, β and ρ parameters are all present in the model of each branch). The n unknown variables can be estimated by means of WLS, where the weight matrix is chosen as the inverse of the covariance matrix of measurements:

$$\boldsymbol{\Sigma}_{\boldsymbol{\epsilon}_{tot}} = \begin{bmatrix}\boldsymbol{\Sigma}_{\boldsymbol{\epsilon}_\Gamma} & \mathbf{0} \\ \mathbf{0} & \boldsymbol{\Sigma}_{\mathbf{e}_{prior}}\end{bmatrix} \tag{9}$$

that includes:

- $\boldsymbol{\Sigma}_{\boldsymbol{\epsilon}_\Gamma} \in \mathbb{R}^{m\times m}$, the covariance matrix of all the equivalent measurements, defined by applying the law of propagation of uncertainty [3] to $\boldsymbol{\Sigma}_{\mathbf{e}_\Gamma}$, the matrix representing the PMU measurement uncertainties, assumed decorrelated for all cases.
$$\boldsymbol{\Sigma}_{\boldsymbol{\epsilon}_\Gamma} = \mathbf{E}_\Gamma \boldsymbol{\Sigma}_{\mathbf{e}_\Gamma} \mathbf{E}_\Gamma^\intercal \tag{10}$$
It is worth pointing out that $\mathbf{E}_\Gamma$ is a rectangular full raw rank matrix, thus $\boldsymbol{\Sigma}_{\boldsymbol{\epsilon}_\Gamma}$ is invertible.
- $\boldsymbol{\Sigma}_{\mathbf{e}_{prior}} \in \mathbb{R}^{n\times n}$ is the diagonal matrix including all the prior variances of the unknowns.

The estimated state vector $\hat{\mathbf{x}}$ is thus the solution of the WLS problem (a subscript is used to recall this):

$$(\mathbf{H}_{tot}^\intercal \mathbf{W}_{tot} \mathbf{H}_{tot})\hat{\mathbf{x}}_{\text{WLS}} = (\mathbf{H}_{tot}^\intercal \mathbf{W}_{tot})\, \mathbf{b}_{tot} \tag{11}$$

where

$$\mathbf{W}_{tot} = \boldsymbol{\Sigma}_{\boldsymbol{\epsilon}_{tot}}^{-1} \tag{12}$$

B. Augmented WLS as Tikhonov Regularization Problem

In the following, it is shown how the estimation method can be framed as a particular case of Tikhonov regularization. This approach provides a way to improve the estimation accuracy by addressing properly multiple loading conditions, which can be commonly observed in power grids, as described in Section III.

The augmented WLS problem (11) can be transformed in a Least Squares (LS) problem by means of the whitening process:

$$\begin{aligned}&\forall\, \mathbf{W}_{\text{Ch}} \in \mathbb{R}^{m\times m} : \mathbf{W}_{\text{Ch}}^\intercal \mathbf{W}_{\text{Ch}} = \boldsymbol{\Sigma}_{\boldsymbol{\epsilon}_\Gamma}^{-1} \\ &\mathbf{b}_{\mathbf{w}} \triangleq \mathbf{W}_{\text{Ch}} \mathbf{b}_\Gamma \Longrightarrow \boldsymbol{\Sigma}_{\mathbf{b}_{\mathbf{w}}} = \mathbf{I}_m\end{aligned} \tag{13}$$

Choosing as whitening matrix $\mathbf{W}_{\text{Ch}} = \mathbf{U}_{\text{Ch}}^{-\intercal}$, where $\mathbf{U}_{\text{Ch}}$ is the upper triangular matrix obtained by means of the Cholesky decomposition of the matrix $\boldsymbol{\Sigma}_{\boldsymbol{\epsilon}_\Gamma}$, and defining $\mathbf{L} = \boldsymbol{\Sigma}_{\mathbf{e}_{prior}}^{-\frac{1}{2}}$ (which is thus a diagonal matrix) the equivalent LS problem is obtained:

$$\hat{\mathbf{x}}_{\text{WLS}} = \arg\min_{\mathbf{x}} \left\| \begin{bmatrix}\mathbf{W}_{\text{Ch}}\mathbf{H}_\Gamma \\ \mathbf{L}\end{bmatrix}\mathbf{x} - \begin{bmatrix}\mathbf{W}_{\text{Ch}}\mathbf{b}_\Gamma \\ \mathbf{0}_{n\times 1}\end{bmatrix} \right\|_2^2 \tag{14}$$

Then, defining

$$\begin{aligned}\mathbf{y} &= \mathbf{L}\mathbf{x} \\ \mathbf{A} &= \mathbf{W}_{\text{Ch}}\mathbf{H}_\Gamma\mathbf{L}^{-1}\end{aligned} \tag{15}$$

and adding the regularization parameter $\mu \in \mathbb{R}^+$, the LS problem becomes:

$$\hat{\mathbf{y}}_\mu = \arg\min_{\mathbf{y}} \left\| \begin{bmatrix}\mathbf{A} \\ \sqrt{\mu}\mathbf{I}_n\end{bmatrix}\mathbf{y} - \begin{bmatrix}\mathbf{b}_{\mathbf{w}} \\ \mathbf{0}_{n\times 1}\end{bmatrix} \right\|_2^2 \tag{16}$$

which is equivalent to the Tikhonov regularization problem in standard form:

$$\hat{\mathbf{y}}_\mu = \arg\min_{\mathbf{y}} \|\mathbf{A}\mathbf{y} - \mathbf{b}_{\mathbf{w}}\|_2^2 + \mu \|\mathbf{y}\|_2^2 \tag{17}$$

as it is immediate to verify by applying the normal equations to (16). Once $\hat{\mathbf{y}}_\mu$ has been estimated, the state $\hat{\mathbf{x}}$ including the desired unknowns can be retrieved with a simple rescaling (inverting the first equation in (15)).

Finally, it is possible to frame the WLS augmented problem (11) as a particular case of the Tikhonov regularization problem where the regularization parameter μ is set to 1 and

$$\hat{\mathbf{x}}_{\text{WLS}} = \mathbf{L}^{-1}\hat{\mathbf{y}}_{\mu=1} \tag{18}$$

thus retrieving the WLS solution from $\hat{\mathbf{y}}_{\mu=1}$ as discussed above.

III. Multiple Operating Cases Management

On one hand, [19] underlines the need to consider multiple measurements in different operating conditions (cases), and [20] highlights the positive effect on line parameter estimation results of using a larger number of constraints. On the other hand, PMUs allow acquiring several measurements per second. The purpose of this section is to show how the management of multiple cases in the estimation process can be optimized, thus taking advantage of the high reporting rate given by PMUs.

A. Estimation Uncertainty Analysis

Equations (16) and (17) address the same problem. While the first is formulated as an augmented LS problem, the second one is formulated as a penalized problem involving two terms:

- $\|\mathbf{A}\mathbf{y} - \mathbf{b}_{\mathbf{w}}\|_2^2$ is the squared norm of the residual vector and is a global index of how well the solution vector $\mathbf{y}$ fits the measurement vector $\mathbf{b}_{\mathbf{w}}$.
- $\|\mathbf{y}\|_2^2$ is the square of the regularization term norm, which takes into account the "energy" of the solution vector $\mathbf{y}$, that is that of the state vector $\mathbf{x}$ weighed with prior information.

In both formulations it is possible to set the regularization parameter μ in order to exploit a-priori information on the

problem to be solved. By applying the normal equations to (16), it follows:

$$\left(\mathbf{A}^{\intercal}\mathbf{A}+\mu\mathbf{I}_n\right)\hat{\mathbf{y}}_\mu=\mathbf{A}^{\intercal}\mathbf{b_w} \tag{19}$$

and by means of the SVD decomposition of the matrix $\mathbf{A}=\mathbf{U}\mathbf{\Sigma}\mathbf{V}^{\intercal}$[1], it is possible to express the analytic solution of the estimation problem as the regularization parameter μ changes:

$$\begin{aligned}\hat{\mathbf{y}}_\mu &= \mathbf{V}\left(\mathbf{\Sigma}^{\intercal}\mathbf{\Sigma}+\mu\mathbf{I}_n\right)^{-1}\mathbf{\Sigma}^{\intercal}\mathbf{U}^{\intercal}\mathbf{b_w}\\ &= \sum_{\sigma_j>0}\mathrm{f}_j\frac{\mathbf{u}^{\intercal}{}_j\mathbf{b_w}}{\sigma_j}\mathbf{v}_j=\sum_{\sigma_j>0}g_j\mathbf{v}_j=\hat{\mathbf{y}}_{\text{Tikhonov}}\end{aligned} \tag{20}$$

where

$$\mathrm{f}_j=\frac{\sigma_j^2}{\sigma_j^2+\mu} \tag{21}$$

while $\mathbf{u}_j$ and $\mathbf{v}_j$ are the jth vectors in $\mathbf{U}$ and $\mathbf{V}$, respectively. The estimate $\hat{\mathbf{y}}_\mu$ is obtained as a linear combination of $\mathbf{v}_j$, $\mathbf{u}^{\mathrm{T}}{}_j\mathbf{b_w}$ are the so-called Fourier coefficients, and f_j is a "low-pass" filter that cuts down components corresponding to $\sigma_j^2 \ll \mu$. Within this framework, it is now possible to investigate the behavior of the estimation algorithm when different cases are available and the effect of selecting different values for μ.

In order to perform such analysis, tests have been carried out on a part of the IEEE 14 bus system [22] shown in Fig. 2, and in particular, on the portion of the network considered in [18], thus on the branches from 1 to 6 and corresponding buses, using the multiple branches approach and the same assumptions that are reported in detail in the following Section IV. The tests have been performed considering different scenarios with different number of cases. To assess the performance of the estimation algorithm, the relative root square error (RRSE) is used:

$$\text{RRSE}=\frac{\|\hat{\mathbf{y}}_\mu-\mathbf{y}\|_2}{\|\mathbf{y}\|_2} \tag{22}$$

Fig. 3 shows the trend in log-log scale of RRSE as a function of $\mu\in[0,...,1000]$ in three different scenarios, using $C\in\{10,50,500\}$ different operating cases respectively. It is important to point out that in [18] only the scenario with $C=10$ was considered. The RRSE values are averaged on $N_{MC}=5000$ Monte Carlo (MC) trials corresponding to different extractions of line parameters and systematic errors. It is clear from the figure that the estimation is completely unreliable when no prior information is used, i.e. when $\mu=0$. The RRSE values drop, reaching a lowland and a minimum value, which is different in the three considered scenarios; for a higher number of cases the minimum is lower and shifted to the right, corresponding thus to a higher μ value (μ_{min} in the following). The flatness of the curve around the minimum means that the algorithm is quite robust with respect

[1] The SVD decomposition of $\mathbf{A}\in\mathbb{R}^{m\times n}$ means that:

$\exists\,\mathbf{U}\in\mathbb{R}^{m\times m}$ and $\mathbf{V}\in\mathbb{R}^{n\times n}:\mathbf{U}^{\intercal}\mathbf{U}=\mathbf{U}\mathbf{U}^{\intercal}=\mathbf{I}_m\in\mathbb{R}^{m\times m}$ and $\mathbf{V}^{\intercal}\mathbf{V}=\mathbf{V}\mathbf{V}^{\intercal}=\mathbf{I}_n\in\mathbb{R}^{n\times n}$

$\exists\,\mathbf{\Sigma}=\mathrm{diag}\left(\sigma_1,\sigma_2,\ldots,\sigma_n\right)\in\mathbb{R}^{m\times n}$ with $\sigma_1\geq\sigma_2\geq\ldots\geq\sigma_n\geq 0:$ $\mathbf{A}=\mathbf{U}\mathbf{\Sigma}\mathbf{V}^{\intercal}$

If $n<m$, the economy size SVD is used, i.e. $\mathbf{A}=\mathbf{U}_n\mathbf{\Sigma}_n\mathbf{V}^{\intercal}$ where $\mathbf{U}_n\in\mathbb{R}^{m\times n}$ (first n columns of $\mathbf{U}$) and $\mathbf{\Sigma}_n\in\mathbb{R}^{n\times n}$ (first n rows of $\mathbf{\Sigma}$).

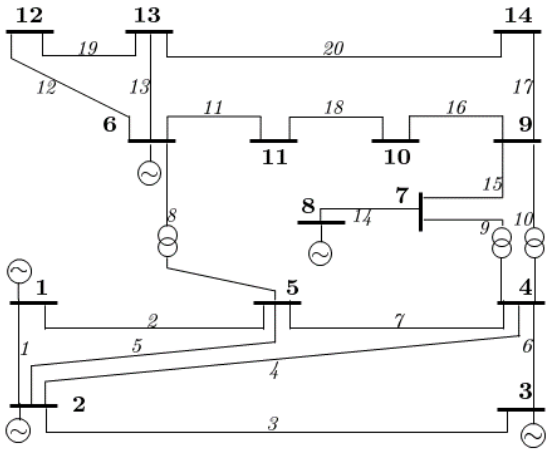

Fig. 2. IEEE 14 bus system.

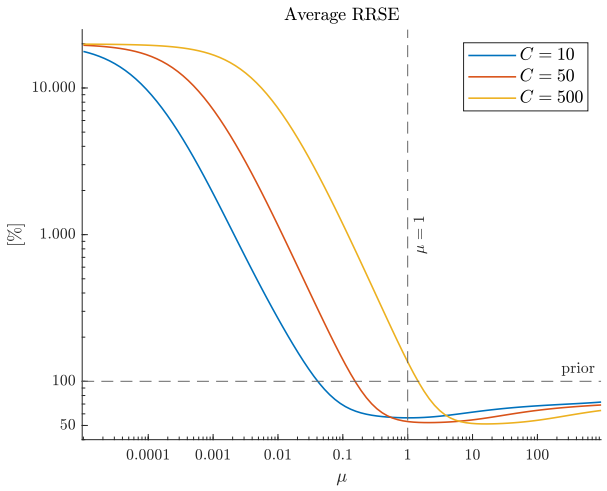

Fig. 3. IEEE 14 - 6 branches, average RRSE as a function of μ with a varying number of operating conditions.

to a-priori information about unknowns. The unreliability of the estimation algorithm for very low μ highlights how the estimation problem starts as under-determined, becomes over-determined exploiting different operating cases [19] but is still not beneficial with larger C without weighting prior information through μ. The vertical dashed line, labeled $\mu=1$, indicates the average RRSE obtained with the WLS approach. It is possible to observe that, when 10 cases are used as in [18], $\mu=1$ is very close to μ_{min} but, when more cases are considered, a greater μ_{min} is needed. Indeed, when 500 cases are considered, the RRSE obtained by means of WLS is greater than 100 %, that is higher than prior error.

Focusing on the causes of this behavior, it is possible to infer that this is not a conditioning problem since, as stated in [19], a higher number of cases leads to a slightly lower condition number. However, the singular values profile significantly shifts towards higher values, thus a greater μ is required to have an appropriate low-pass filter effect through (21), which is needed to satisfy the discrete Picard condition [23], [24]. The Picard condition states that the Fourier coefficients in (20)

should decrease faster than the corresponding singular values σ_j in order to have a limited solution in (16). In this regard, it is thus possible to use this framework for a more accurate estimation, as explained in the following.

B. Proposed Method and Regularization

The proposed approach is to use a value of μ which is tuned to the needs of the problems at hand and depends on its parameters. Tests conducted with different configurations have shown that σ_j values increase with the square root of the number of constraints embodied in the measurement matrix $\mathbf{A}$. For this reason, the regularization parameter has been empirically chosen as:

$$\mu_{sqrt} = \sqrt{\frac{m}{n}} \tag{23}$$

to take into account the singular values trend. Fig. 4 shows the Picard condition plots relative to the scenario with $C = 500$: the red circle indicates the ideal solution, i.e. without measurement errors, while the purple, blue and green asterisks represent g_j coefficients obtained with no prior ($\mu = 0$), with WLS ($\mu = 1$) and with the proposed μ_{sqrt}, respectively. It is possible to observe how the proposed regularization parameter μ is more effective than the previous ones in containing the coefficients.

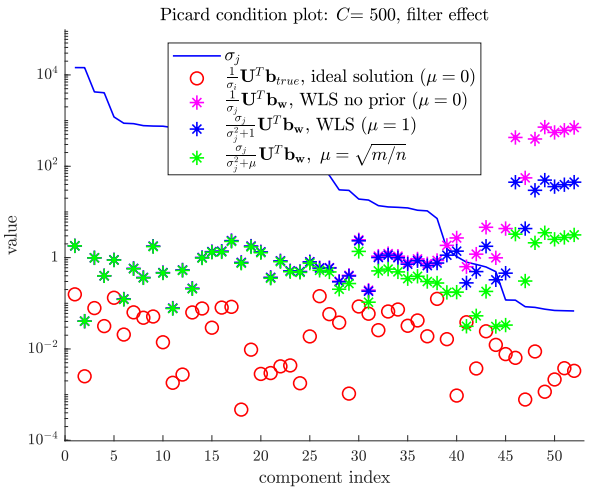

Fig. 4. IEEE 14 - 6 branches, filtering effect.

The proposed method has been compared with the classical algorithms for the choice of the regularization parameter in the Tikhonov problem: the *L-curve* criterion (LCC), the *Generalized Cross Validation* (GCV) and the *Discrepancy Principle* (DP) [23], [25]. The *L-curve* is a useful graphical tool [25] consisting in a log-log plot of the regularization term norm versus the relative residual term norm, for all the considered μ. The resulting curve assumes the aspect of an L (hence the name). LCC selects as best regularization parameter the corner value with the motivation that it represents a good trade-off between the two terms involved in the penalized formulation (17). The GCV is instead a statistically based approach. For both LCC and GCV the implementations of [23] are here used.

DP [26] is the only method based on the knowledge of the error norm and suggests choosing the μ value so that the residual norm is close to the error norm. Thus:

$$\mu_{\text{DP}} : \left\|\mathbf{b}_{\mathbf{w}} - \mathbf{A}\hat{\mathbf{y}}_{\mu_{\text{DP}}}\right\|_2 \approx \tau \left\|\boldsymbol{\epsilon}_{\mathbf{w}}\right\|_2, \ \tau \geq 1 \tag{24}$$

where $\boldsymbol{\epsilon}_{\mathbf{w}} = \mathbf{W}_{\text{Ch}}\boldsymbol{\epsilon}_{\Gamma}$ is the whitened measurement error vector, having the identity matrix as covariance matrix. In order to obtain a suitable estimation of the measurement error norm, the method illustrated in [27] has been used and adapted to the specific problem. To solve (24), the method described in [28] has been followed (see Appendix B).

Moreover, in order to have a benchmark for the performance of the estimation algorithm within the Tikhonov regularization problem framework, the optimal μ for each MC trial, defined as

$$\mu_{opt} = \arg\min_{\mu} \text{RRSE} \tag{25}$$

has been also used. As clear from the definition, μ_{opt} is used only as a reference and it is not available in practice since its computation requires prior knowledge of $\mathbf{y}$ (true values).

Fig. 5 shows the average RRSE trends when C is changing from 10 to 500. The RRSE of WLS method, corresponding to $\mu = 1$, improves at the beginning reaching a minimum with about 50 cases, then increases becoming soon unreliable for a high number of cases (see also Fig. 3). The classical regularization methods (LCC, GCV, DP) are unable to reach good estimation performance since the underlying problem is not due to conditioning issues and, consequently, the regularization parameters selected by means of these criteria lead to a too strong low-pass filter effect. Finally, the figure shows that the proposed selection method μ_{sqrt} in (23) is close to the performance of the benchmark μ_{opt}.

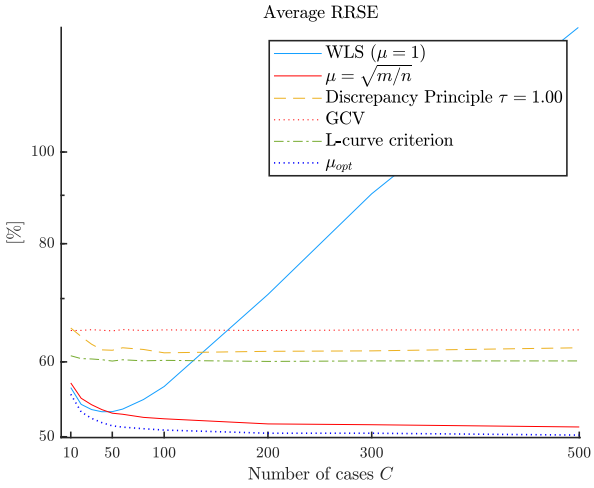

Fig. 5. IEEE 14 - 6 branches: average RRSE (5000 MC trials performed) when different numbers of operating conditions are considered.

A flow chart schematically representing the proposal is shown in Fig. 6. Finally, some remarks on the computational cost of the proposed method are reported in the following. There are two important points to consider, i.e. the construction of the whitening matrix $\mathbf{W}_{\text{Ch}}$ and the SVD decomposition of $\mathbf{A}$. To reduce the computational cost, the whitening matrix

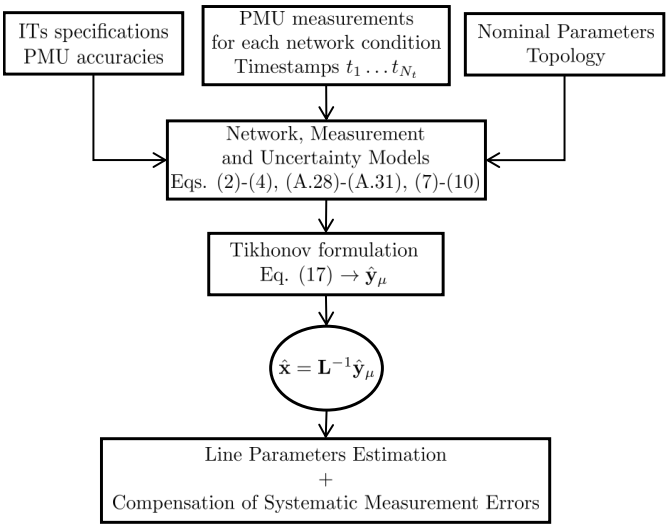

Fig. 6. Flow chart of the proposed procedure.

is built from blocks, that is performing the Cholesky factorization of the small submatrices of $\mathbf{\Sigma}_{\boldsymbol{\epsilon}_\Gamma}$ corresponding to each case, inverting the computed small triangular matrices and finally integrating blocks. Even if the row size of $\mathbf{A}$ increases with C, $\mathbf{A}$ becomes a very slim matrix ($n \ll m$) and the economy size SVD (see footnote 1) allows a fast computation.

IV. Tests and Results

In this Section, performance evaluation tests are reported to assess the validity of the proposed approach. All tests have been carried out using the IEEE 14 bus system [22] shown in Fig. 2. Classical regularization methods are compared with the proposed one (as discussed in Section III-B) and different number of involved branches are used. Tests have been performed on $C \in \{10, 20, ..., 1000\}$ cases (as mentioned before, to take into account different network conditions) and $M = 10$ repeated measurements for each case. $N_{MC} = 5000$ trials have been used to validate statistically the results.

For each MC trial, different systematic errors have been simulated. Systematic errors are attributed to the ITs, thus depending on their accuracy class, whereas random errors are considered associated with the PMUs. For each measurement instant and each case, random errors are extracted and added, together with the systematic errors of the considered trial, to the powerflow reference voltages and currents to obtain both magnitude and phase angle synchrophasor measurements. The following assumptions are used in the tests, in order to have a realistic set-up:

1) Maximum deviations of line parameters R_{ij}, X_{ij} and $B_{sh,ij}$ have been assumed equal to $\pm 15\,\%$.
2) ITs are assumed to be of class 0.5, thus using $0.5\,\%$ for maximum voltage and current ratio errors, 0.9 crad for maximum CT phase-angle displacement and 0.6 crad for maximum VT phase-angle displacement. For every test in the following, the errors have been extracted from uniform distributions to define the actual systematic errors for each MC trial.
3) For the errors associated with PMUs, a maximum amplitude error of $0.1\,\%$ and a maximum phase angle error of 0.1 crad (10^{-3} rad) are used.
4) Load/generator variability of $\pm 10\,\%$ with respect to nominal values (for both active and reactive powers) among different cases is considered.

To assess the performance of both the estimation of the line parameters and the compensation of systematic errors, the root mean square error (RMSE) is used:

$$\text{RMSE} = \sqrt{\sum_{i=1}^{N_{MC}} \frac{(\hat{\nu} - \nu)^2}{N_{MC}}} \tag{26}$$

where $\hat{}$ indicates the estimated quantity. In (26) ν is a placeholder for each unknown in $\mathbf{x}$ and can thus be (considering a generic branch (i,j)) equal to $\xi_i^{sys}, \alpha_i^{sys}, \xi_j^{sys}, \alpha_j^{sys}, \eta_{ij}^{sys}, \psi_{ij}^{sys}, \eta_{ji}^{sys}, \psi_{ji}^{sys}, \gamma_{ij}, \beta_{ij}$ or ρ_{ij}. In the following, for the sake of simplicity, each branch will be indicated with a single index k as in Fig. 2 and thus the associated parameters will be $\gamma_k, \beta_k, \rho_k$.

A. Estimation on a Set of Selected Branches

The first series of tests is conducted on a part of the IEEE 14 network, on the high voltage nodes from 1 to 5, considering the multi-branch approach. The tests have been carried out using all the methods presented in Section III but, according to the analysis summarized in the Fig. 5, from here on the results are mainly focused on the comparison of the performance of the WLS ($\mu = 1$, [18]) with the proposed method (μ_{sqrt}-method). The performance with the ideal μ_{opt} value in each trial is also considered as an upper bound. Both results, WLS and μ_{sqrt}-method, are presented choosing the best scenario for each method, i.e. the value of C that allows best performance (C_{best})[2]. In addition, the basic scenario $C = 10$ is also used with the WLS method to have a clear comparison with the multi-branch estimation results presented in [18]. Table I reports the considered scenarios and the corresponding RRSE results averaged among 5000 trials.

In the following, all the estimation results presented in terms of RMSE for a specific unknown must be compared with the corresponding prior standard deviation. Considering the systematic measurement errors, the prior standard deviation is $\Delta_\xi/\sqrt{3} = \Delta_\eta/\sqrt{3} \simeq 0.29\,\%$ for the amplitude error of voltage and current measurements, respectively (Δ indicates the maximum deviation), $\Delta_\alpha/\sqrt{3} \simeq 0.35$ crad and $\Delta_\psi/\sqrt{3} \simeq 0.52$ crad for the phase displacement error of voltage and current measurements, respectively. Considering network parameters, the standard deviation of the relative errors is $\Delta_\gamma/\sqrt{3} = \Delta_\beta/\sqrt{3} = \Delta_\rho/\sqrt{3} \simeq 8.66\,\%$.

In Fig. 7, the RMSE results for the branch resistance estimations are reported, considering the scenarios of Table I. It is possible to notice that the results obtained according to [18] (green plus signs) can be improved on average of about $32.2\,\%$ when the same WLS configuration is used but with 40 cases (blue plus signs). However, the best WLS configuration is outperformed by the proposed regularization method (red

[2]The ideal results with μ_{opt} are presented using the same C as μ_{sqrt}.

asterisks), with an additional average improvement of 25.5 %. It has to be mentioned also that, in this case, the μ_{sqrt}-method is very close to μ_{opt} results. It is important to highlight that RRSE is a summary index that considers all the errors on the unknown parameters together (see (22) and (25)). For this reason, the RMSEs achieved with μ_{opt}, only for some specific quantities or some branches, might not be the lowest. This is the case of Fig. 7, where μ_{sqrt}-method is even slightly better for γ, but for other unknowns (see ξ-related results in the following) μ_{opt} is more accurate.

The comprehensive picture of line parameters estimation is shown in Fig. 8 where all parameter types are considered. It is clear that the proposed method (bars in foreground with solid line edge) significantly improves the best WLS results (bars in background with dash-dotted edge) for all the line parameters and for all the branches. The average improvements (percent error reduction) are 34.9 % and 57.2 % for β_k and ρ_k, respectively.

TABLE I
IEEE 14 - 6 BRANCHES: BEST AVERAGE RRSE (5000 MC TRIALS) FOR DIFFERENT METHODS

Method	Average RRSE [%]
WLS ($\mu = 1$), $C = 10$ [18]	56.35
WLS ($\mu = 1$), $C_{best} = 40$	53.14
$\mu = \sqrt{m/n}$, $C_{best} = 500$	51.21
μ_{opt}, $C = 500$	50.20

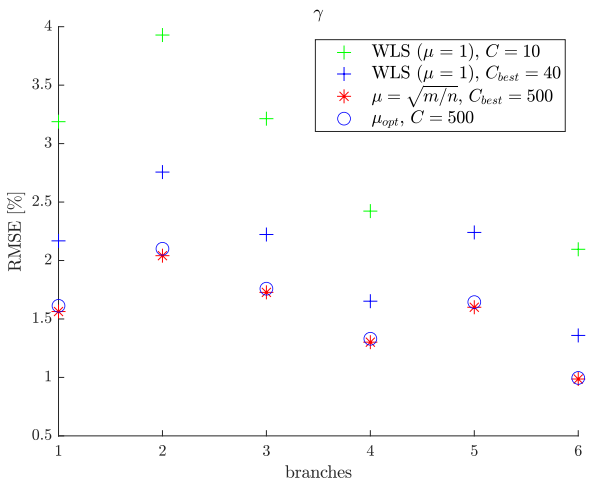

Fig. 7. IEEE 14 - 6 branches: estimation results for γ parameters.

The RMSE results for ξ estimation, which represent the voltage magnitude compensation performance, are shown in Fig. 9 as a function of C for all the regularization methods presented in Section III. It is possible to highlight that the results of WLS (green plus signs) and, for more than 50 cases, DP with $\tau = 1.00$ (blue triangles) tend to diverge significantly, going even beyond prior values (black dashed line). In particular, WLS method can lead to unreliable results when the number of cases increases, confirming the results previously shown in Figures 3 and 5.

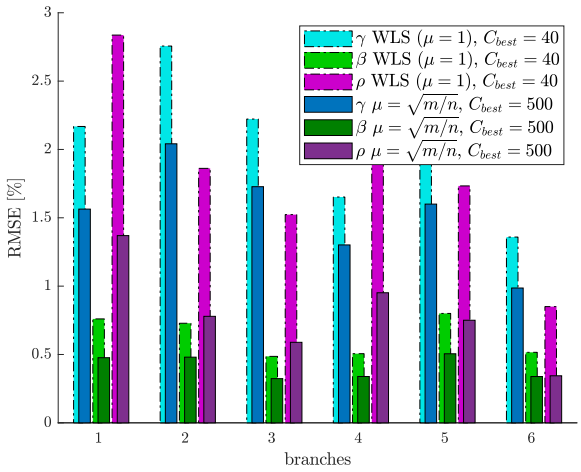

Fig. 8. IEEE 14 - 6 branches: estimation results for all line parameters.

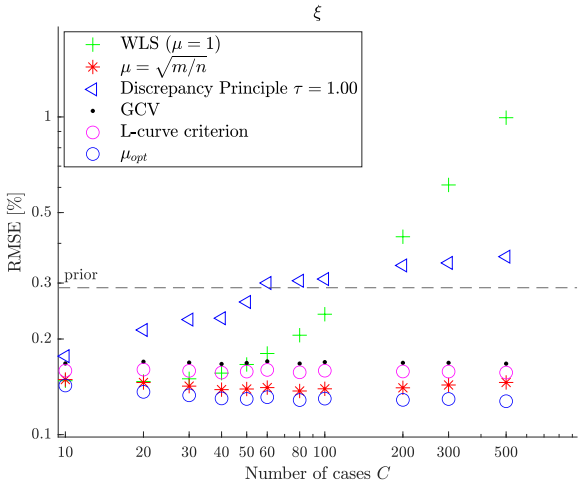

Fig. 9. IEEE 14 - 6 branches: ξ estimation results as a function of the number of cases for all the considered methods.

The considerations drawn for multi-branch approach are similar to those that can be derived for the single-branch case (see [18]). Table II reports, for example, a comparison of the RMSE for ξ_1 when both $\mu = 1$ and $\mu = \sqrt{m/n}$ are used with $C = 10, 500$. While confirming the significant enhancement of the multi-branch method (see Fig. 4 in [18]), Table II shows that the regularization brings clear benefits when C is high also in the single-branch approach and prevents from critical conditions for ξ as those already identified in Fig. 9.

TABLE II
IEEE 14 - NODE 1: RMSE (5000 MC TRIALS) FOR ξ_1 - COMPARISON BETWEEN MULTI-BRANCH AND SINGLE-BRANCH APPROACHES

Method	C	RMSE [%]	
		Multi-branch	Single-branch
$\mu = \sqrt{m/n}$	10	0.16	0.22
$\mu = \sqrt{m/n}$	500	0.16	0.21
WLS ($\mu = 1$)	10	0.16	0.22
WLS ($\mu = 1$)	500	1.01	0.46

B. Estimation on the Entire Network

Further analyses have been carried out on the entire IEEE 14 bus test network using the multiple branches approach. Several scenarios have been simulated considering a variable number of cases ($C \in \{10, 20, ..., 1000\}$) and comparing WLS and μ_{sqrt} methods. For both methods, the best scenario is selected as done in previous tests: C_{best} depends on the configuration. In particular, repeating the analysis and optimization according to Section III on the entire network, it results $C_{best} = 30$ for WLS and $C_{best} = 200$ for μ_{sqrt}-method. Fig. 10 shows the RMSEs for β_k estimations (focusing on $k = \{1, ..., 6\}$, i.e. the reactance of the branches from 1 to 6) evaluated with the two methods and two different multi-branch measurement matrices: the first one is obtained using only the constraints due to the first 6 branches ($l = 6$), while the second one embodies the constraints of the entire network ($l = 20$). The results obtained in [18] using the WLS with $C = 10$ cases are reported with the green plus signs. The figure shows the benefits of exploiting in a suitable way a greater number of constraints, which are due to both a larger number of cases and a wider set of monitored branches. It is also possible to highlight that the average improvement going from the WLS as applied in [18] to the best results obtained with $\mu = \sqrt{m/n}$, $C_{best} = 200$ and considering the entire network (blue asterisks) is of about 66.6 %.

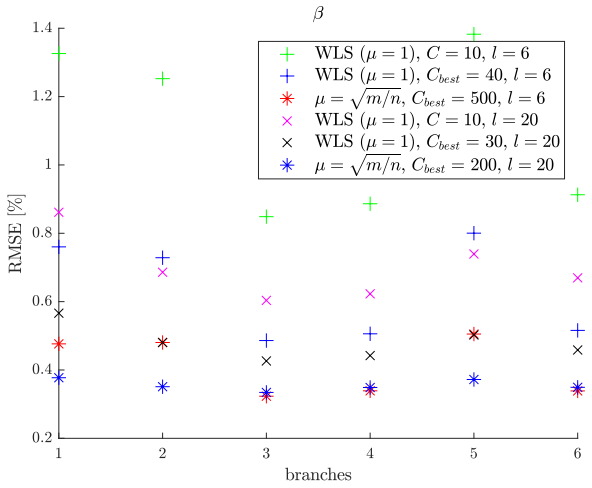

Fig. 10. β estimation results with multi-branch approach applied to a portion and to the entire network using different methods and configurations.

Fig. 11 shows the RMSE results for all the line parameters obtained on the entire network using only C_{best} for the WLS (top figure) and μ_{sqrt}-method (bottom figure). It is important to underline that in the tests all the branches are analyzed and thus also branches that can be modeled using line reactance only or neglecting shunt susceptance are taken into account (some parameters are thus not present in the figure). A significantly better estimation can be achieved with the proposed regularization method. In fact, γ_k, β_k and ρ_k estimations have an average improvement of 16 %, 23.9 % and 44.4 %, respectively.

Finally, even though an all-embracing comparison with other algorithms from the literature is not possible, an example of the RMSE results achievable with different methods using the same measurements is reported in Table III. Two methods have been compared with the proposed one, which is summarized in Fig. 6. In particular, the first method is a direct estimation method (Method A) for the line parameters based on the equations in [5] (the same equations can be found in [6]). For a fair comparison, the estimates obtained for a single case have been averaged and repeated measurements are considered as in the proposed method. The second one is the method presented in [17, Sec. IV] (Method B), which is intended to estimate the parameters of a line and the compensation factors for the ITs at the arrival node. Two C values have been used: $C = 10$ is the base value while $C = 200$ corresponds to previous tests in this section. Branch 1 of the network is chosen for the comparison, but similar results can be found on the other branches. Table III reports the RMSE results for the resistance and reactance and for the systematic errors of the measurements of the end node. Method A does not allow estimating the systematic errors and Method B does not allow computing the systematic errors at the start node of the branch (thus, the corresponding RMSEs are not reported for the proposed method either). To test also the robustness of the method, PMU accuracy has been changed with respect to previous tests. In particular, a maximum amplitude error and a maximum phase-angle error of 0.2 % and 0.2 crad, respectively, have been also tested.

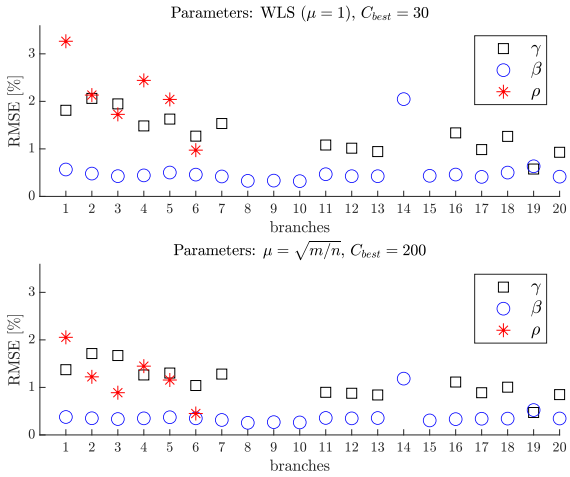

Fig. 11. IEEE 14 - entire network: estimation results for all the line parameters.

The results in Table III show that the proposed method is significantly more accurate than the others in every considered condition and configuration. Method A is always worse than prior values for γ_1, since systematic errors strongly affect its estimates. It is interesting to notice that its RMSEs vary only slightly with C and PMU accuracy, because systematic errors are the main source of estimation errors. Method B takes advantage of the number of used cases to reduce the line parameter errors but RMSEs of systematic errors on voltage and current measurements are always equal to or larger than prior values. In addition, the proposed method is more robust than Method B when PMU uncertainty increases,

as it is highlighted by the case with PMU accuracy ($0.2\,\%$, $0.2\,\text{crad}$) and $C = 10$. These and other results have shown that considering all the uncertainty sources and using a multi-branch approach is key to improve performance.

TABLE III
IEEE 14 - BRANCH 1: COMPARISON BETWEEN DIFFERENT METHODS

Method	C	PMU accuracy $\lvert\cdot\rvert[\%], \angle[\text{crad}]$	RMSE γ_1 [%]	β_1 [%]	ξ_2 [%]	α_2 [crad]	η_{21} [%]	ψ_{21} [crad]
Proposed Method	10	0.1, 0.1	2.53	0.88	0.10	0.10	0.20	0.37
		0.2, 0.2	3.73	1.53	0.11	0.14	0.21	0.38
	200	0.1, 0.1	1.38	0.38	0.10	0.09	0.20	0.36
		0.2, 0.2	2.08	0.76	0.11	0.11	0.20	0.37
Method A [5]	10	0.1, 0.1	13.15	5.16	-	-	-	-
		0.2, 0.2	13.16	5.16	-	-	-	-
	200	0.1, 0.1	13.08	5.10	-	-	-	-
		0.2, 0.2	13.08	5.10	-	-	-	-
Method B [17, Sec. IV]	10	0.1, 0.1	7.34	2.48	0.37	0.42	0.36	0.56
		0.2, 0.2	14.99	5.71	0.55	0.65	0.53	0.68
	200	0.1, 0.1	2.55	0.97	0.29	0.36	0.29	0.53
		0.2, 0.2	4.84	3.05	0.31	0.46	0.30	0.53

V. CONCLUSIONS

The paper has presented a multiple branches method to estimate simultaneously the line parameters in the transmission lines and the systematic errors in synchronized phasor measurements, which is enhanced in the presence of multiple measurement sets obtained from a wide area measurement system and corresponding to multiple timestamps. The proposed method improves the information needed for an effective management of the transmission network based on a comprehensive definition of the uncertainty model. The adopted model allows taking into account the different error contributions in a realistic measurement chain and prior information on the accuracy of ITs and PMUs, e.g. that achievable from instrument datasheets and characterization procedures, can also be successfully exploited. The method has been designed within the framework of Tikhonov regularization, thus allowing an optimization of the algorithm and the definition of a configuration criterion for the specific problem. This generalization allows exploiting the potentialities of PMUs, that is high accuracy and reporting rate, to improve the estimation of line parameters and to refine the compensation of systematic measurement errors when multiple measurement sets are available. Simulation tests performed using the standard IEEE 14 bus system have confirmed the validity of the proposed approach and have highlighted the benefits of estimating all the unknowns together in the proposed multiple branches approach.

APPENDIX A
DERIVATION OF THE MEASUREMENT MATRIX AND OF THE UNCERTAINTY REPRESENTATION

Assuming that the absolute values of all the errors are low, much lower than one (i.e. $|\xi|, |\alpha|, |\eta|, |\psi| \ll 1$), which is realistic for typical transducer and PMU accuracies, equations in (1) can be rewritten so that v_h^R and i_{ij}^R are expressed as functions of measured synchrophasors v_h and i_{ij} as follows:

$$\begin{aligned} v_h^R &\simeq \left(1 - \xi_h^{sys} - \xi_h^{rnd}\right)\left(V_h^r + jV_h^x\right) \\ &\quad \cdot \left(1 - j\alpha_h^{sys} - j\alpha_h^{rnd}\right) \\ i_{ij}^R &\simeq \left(1 - \eta_{ij}^{sys} - \eta_{ij}^{rnd}\right)\left(I_{ij}^r + jI_{ij}^x\right) \\ &\quad \cdot \left(1 - j\psi_{ij}^{sys} - j\psi_{ij}^{rnd}\right) \end{aligned} \tag{A.27}$$

where, using the approximation $(1+x)^{-1} \simeq 1 - x$ for $x \simeq 0$, the amplitude errors that would be at the denominator on the right side are brought at the numerator. Using the approximation $e^{-jx} \simeq 1 - jx$, the exponential functions in (1) can be first conjugated and then linearized to find (A.27).

Using (1) and (4) in (2) and (3), neglecting second order terms and splitting real and imaginary parts of the equations, equations (A.28)-(A.31) (on the top of the next page) are obtained. In each equation, the first term depends on known quantities (measured and nominal values) and the second term is a linear combination of systematic and random errors, where the coefficients are given again by measured and nominal values.

APPENDIX B
DISCREPANCY PRINCIPLE APPLICATION

The square residual norm term in (17) can be rewritten as:

$$\begin{aligned} \|\mathbf{b_w} - \mathbf{A}\hat{\mathbf{y}}_\mu\|_2^2 &= \left\|\mathbf{b_w} - \mathbf{A}(\mathbf{A}^\intercal\mathbf{A} + \mu\mathbf{I}_n)^{-1}\mathbf{A}^\intercal\mathbf{b_w}\right\|_2^2 \\ &= \left\|(\mathbf{I}_m - \mathbf{\Sigma}(\mathbf{\Sigma}^\intercal\mathbf{\Sigma} + \mu\mathbf{I}_n)^{-1}\mathbf{\Sigma}^\intercal)\mathbf{U}^\intercal\mathbf{b_w}\right\|_2^2 \\ &= \sum_{\sigma_j>0}\left(\left(1 - \frac{\sigma_j^2}{\sigma_j^2+\mu}\right)\mathbf{u}_j^\intercal\mathbf{b_w}\right)^2 \\ &= \sum_{\sigma_j>0}\left(\frac{\mathbf{u}_j^\intercal\mathbf{b_w}}{\chi\sigma_j^2+1}\right)^2 \end{aligned} \tag{B.32}$$

where $\chi \triangleq \frac{1}{\mu}$. Then, considering that

$$\Psi(\chi) = \sum_{\sigma_j>0}\left(\frac{\mathbf{u}_j^\intercal\mathbf{b_w}}{\chi\sigma_j^2+1}\right)^2 - \tau^2\|\boldsymbol{\epsilon}_\mathbf{w}\|_2^2 \tag{B.33}$$

is a monotone decreasing function that changes sign (starting positive for $\chi = 0$ and for reasonable values of the error vector norm and becoming negative as χ increases), a zero crossing point exists and can be found by the Newton method [28].

REFERENCES

[1] G. Kusic and D. Garrison, "Measurement of transmission line parameters from SCADA data," in *IEEE PES Power Systems Conference and Exposition*, Oct. 2004, pp. 344–349.

[2] H. Zhang, Z. Diao, and Y. Cui, "Identification of Power Network Branch Parameters Based on State Space Transformation," *IEEE Access*, vol. 7, pp. 91 720–91 730, Jul. 2019.

[3] "Evaluation of data - guide to the expression of uncertainty in measurement," *JCGM 100:2008*, Sep. 2008.

[4] J. Fu, G. Song, and B. De Schutter, "Influence of Measurement Uncertainty on Parameter Estimation and Fault Location for Transmission Lines," *IEEE Trans. Autom. Sci. Eng.*, vol. 18, no. 1, pp. 337–345, Jan. 2021.

$$
\begin{aligned}
V_i^r - V_j^r - I_{ij}^r R_{ij}^0 + I_{ij}^x X_{ij}^0 - \tfrac{B_{sh,ij}^0}{2}\left(V_i^r X_{ij}^0 + V_i^x R_{ij}^0\right) \simeq{}& \left[V_i^r - \tfrac{B_{sh,ij}^0}{2}\left(V_i^r X_{ij}^0 + V_i^x R_{ij}^0\right)\right]\left(\xi_i^{sys} + \xi_i^{rnd}\right) \\
&+ \left[-V_i^x - \tfrac{B_{sh,ij}^0}{2}\left(V_i^r R_{ij}^0 - V_i^x X_{ij}^0\right)\right]\left(\alpha_i^{sys} + \alpha_i^{rnd}\right) - V_j^r\left(\xi_j^{sys} + \xi_j^{rnd}\right) + V_j^x\left(\alpha_j^{sys} + \alpha_j^{rnd}\right) \\
&+ \left(-I_{ij}^r R_{ij}^0 + I_{ij}^x X_{ij}^0\right)\left(\eta_{ij}^{sys} + \eta_{ij}^{rnd}\right) + \left(I_{ij}^r X_{ij}^0 + I_{ij}^x R_{ij}^0\right)\left(\psi_{ij}^{sys} + \psi_{ij}^{rnd}\right) \\
&+ R_{ij}^0\left(I_{ij}^r + \tfrac{B_{sh,ij}^0}{2} V_i^x\right)\gamma_{ij} + X_{ij}^0\left(-I_{ij}^x + \tfrac{B_{sh,ij}^0}{2} V_i^r\right)\beta_{ij} + \frac{B_{sh,ij}^0}{2}\left(V_i^r X_{ij}^0 + V_i^x R_{ij}^0\right)\rho_{ij}
\end{aligned}
\tag{A.28}
$$

$$
\begin{aligned}
V_i^x - V_j^x - I_{ij}^r X_{ij}^0 - I_{ij}^x R_{ij}^0 + \tfrac{B_{sh,ij}^0}{2}\left(V_i^r R_{ij}^0 - V_i^x X_{ij}^0\right) \simeq{}& \left[V_i^x + \tfrac{B_{sh,ij}^0}{2}\left(V_i^r R_{ij}^0 - V_i^x X_{ij}^0\right)\right]\left(\xi_i^{sys} + \xi_i^{rnd}\right) \\
&+ \left[V_i^r + \tfrac{B_{sh,ij}^0}{2}\left(-V_i^r X_{ij}^0 + V_i^x R_{ij}^0\right)\right]\left(\alpha_i^{sys} + \alpha_i^{rnd}\right) - V_j^x\left(\xi_j^{sys} + \xi_j^{rnd}\right) - V_j^r\left(\alpha_j^{sys} + \alpha_j^{rnd}\right) \\
&+ \left(-I_{ij}^r X_{ij}^0 - I_{ij}^x R_{ij}^0\right)\left(\eta_{ij}^{sys} + \eta_{ij}^{rnd}\right) + \left(-I_{ij}^r R_{ij}^0 + I_{ij}^x X_{ij}^0\right)\left(\psi_{ij}^{sys} + \psi_{ij}^{rnd}\right) \\
&+ R_{ij}^0\left(I_{ij}^x - \tfrac{B_{sh,ij}^0}{2} V_i^r\right)\gamma_{ij} + X_{ij}^0\left(I_{ij}^r + \tfrac{B_{sh,ij}^0}{2} V_i^x\right)\beta_{ij} + \frac{B_{sh,ij}^0}{2}\left(V_i^x X_{ij}^0 - V_i^r R_{ij}^0\right)\rho_{ij}
\end{aligned}
\tag{A.29}
$$

$$
\begin{aligned}
I_{ij}^r + I_{ji}^r + \frac{B_{sh,ij}^0}{2}\left(V_i^x + V_j^x\right) \simeq{}& I_{ij}^r\left(\eta_{ij}^{sys} + \eta_{ij}^{rnd}\right) - I_{ij}^x\left(\psi_{ij}^{sys} + \psi_{ij}^{rnd}\right) + I_{ji}^r\left(\eta_{ji}^{sys} + \eta_{ji}^{rnd}\right) - I_{ji}^x\left(\psi_{ji}^{sys} + \psi_{ji}^{rnd}\right) \\
&+ \tfrac{B_{sh,ij}^0}{2}\left[V_i^x\left(\xi_i^{sys} + \xi_i^{rnd}\right) + V_j^x\left(\xi_j^{sys} + \xi_j^{rnd}\right) + V_i^r\left(\alpha_i^{sys} + \alpha_i^{rnd}\right) + V_j^r\left(\alpha_j^{sys} + \alpha_j^{rnd}\right) - \left(V_i^x + V_j^x\right)\rho_{ij}\right]
\end{aligned}
\tag{A.30}
$$

$$
\begin{aligned}
I_{ij}^x + I_{ji}^x - \frac{B_{sh,ij}^0}{2}\left(V_i^r + V_j^r\right) \simeq{}& I_{ij}^x\left(\eta_{ij}^{sys} + \eta_{ij}^{rnd}\right) + I_{ij}^r\left(\psi_{ij}^{sys} + \psi_{ij}^{rnd}\right) + I_{ji}^r\left(\eta_{ji}^{sys} + \eta_{ji}^{rnd}\right) + I_{ji}^x\left(\psi_{ji}^{sys} + \psi_{ji}^{rnd}\right) \\
&+ \tfrac{B_{sh,ij}^0}{2}\left[-V_i^r\left(\xi_i^{sys} + \xi_i^{rnd}\right) - V_j^r\left(\xi_j^{sys} + \xi_j^{rnd}\right) + V_i^x\left(\alpha_i^{sys} + \alpha_i^{rnd}\right) + V_j^x\left(\alpha_j^{sys} + \alpha_j^{rnd}\right) + \left(V_i^r + V_j^r\right)\rho_{ij}\right]
\end{aligned}
\tag{A.31}
$$

[5] M. Asprou, E. Kyriakides, and M. M. Albu, "Uncertainty Bounds of Transmission Line Parameters Estimated From Synchronized Measurements," *IEEE Trans. Instrum. Meas.*, vol. 68, no. 8, pp. 2808–2818, Aug. 2019.

[6] S. Vlahinic, D. Frankovic, M. Z. Durovic, and N. Stojkovic, "Measurement Uncertainty Evaluation of Transmission Line Parameters," *IEEE Trans. Instrum. Meas.*, vol. 70, pp. 1–7, Apr. 2021.

[7] A. Xue, F. Xu, K. E. Martin, H. You, J. Xu, L. Wang, and G. Wei, "Robust Identification Method for Transmission Line Parameters That Considers PMU Phase Angle Error," *IEEE Access*, vol. 8, pp. 86 962–86 971, May 2020.

[8] V. Milojević, S. Čalija, G. Rietveld, M. V. Ačanski, and D. Colangelo, "Utilization of pmu measurements for three-phase line parameter estimation in power systems," *IEEE Trans. Instrum. Meas.*, vol. 67, no. 10, pp. 2453–2462, Oct. 2018.

[9] M. Asprou and E. Kyriakides, "Identification and estimation of erroneous transmission line parameters using pmu measurements," *IEEE Trans. Power Del.*, vol. 32, no. 6, pp. 2510–2519, Dec. 2017.

[10] A. Wehenkel, A. Mukhopadhyay, J.-Y. L. Boudec, and M. Paolone, "Parameter Estimation of Three-Phase Untransposed Short Transmission Lines From Synchrophasor Measurements," *IEEE Trans. Instrum. Meas.*, vol. 69, no. 9, pp. 6143–6154, Sep. 2020.

[11] Z. Wu, L. T. Zora, and A. G. Phadke, "Simultaneous transmission line parameter and PMU measurement calibration," in *2015 IEEE Power & Energy Society General Meeting*, Denver, CO, USA, Jul. 2015, pp. 1–5.

[12] Y. G. Kononov, O. S. Rybasova, and K. A. Sidirov, "Identification of overhead-line parameters from pmu data with compensation of systematic measurement errors," in *2018 International Conference on Industrial Engineering, Applications and Manufacturing (ICIEAM)*, Moscow, Russia, May 2018, pp. 1–5.

[13] R. S. Singh, S. Babaev, V. Cuk, S. Cobben, and H. van den Brom, "Line Parameters Estimation in Presence of Uncalibrated Instrument Transformers," in *2019 2nd International Colloquium on Smart Grid Metrology (SMAGRIMET)*, Split, Croatia, Apr. 2019, pp. 1–8.

[14] A. Pal, P. Chatterjee, J. S. Thorp, and V. A. Centeno, "Online Calibration of Voltage Transformers Using Synchrophasor Measurements," *IEEE Trans. Power Del.*, vol. 31, no. 1, pp. 370–380, Feb. 2016.

[15] C. Wang, V. A. Centeno, K. D. Jones, and D. Yang, "Transmission Lines Positive Sequence Parameters Estimation and Instrument Transformers Calibration Based on PMU Measurement Error Model," *IEEE Access*, vol. 7, pp. 145 104–145 117, Oct. 2019.

[16] K. V. Khandeparkar, S. A. Soman, and G. Gajjar, "Detection and Correction of Systematic Errors in Instrument Transformers Along With Line Parameter Estimation Using PMU Data," *IEEE Trans. Power Syst.*, vol. 32, no. 4, pp. 3089–3098, Jul. 2017.

[17] H. Goklani, G. Gajjar, and S. A. Soman, "Instrument transformer calibration and robust estimation of transmission line parameters using pmu measurements," *IEEE Trans. Power Syst.*, vol. 36, no. 3, pp. 1761–1770, May 2021.

[18] C. Muscas, P. A. Pegoraro, C. Sitzia, A. V. Solinas, and S. Sulis, "Compensation of systematic measurement errors in pmu-based monitoring systems for transmission grids," in *2021 IEEE International Instrumentation and Measurement Technology Conference (I2MTC)*, Glasgow, UK, May 2021, pp. 1–6.

[19] P. Ren, H. Lev-Ari, and A. Abur, "Tracking Three-Phase Untransposed Transmission Line Parameters Using Synchronized Measurements," *IEEE Trans. Power Syst.*, vol. 33, no. 4, pp. 4155–4163, Jul. 2018.

[20] P. A. Pegoraro, K. Brady, P. Castello, C. Muscas, and A. von Meier, "Line impedance estimation based on synchrophasor measurements for power distribution systems," *IEEE Trans. Instrum. Meas.*, vol. 68, no. 4, pp. 1002–1013, Apr. 2019.

[21] P. A. Pegoraro, K. Brady, P. Castello, C. Muscas, and A. von Meier, "Compensation of systematic measurement errors in a pmu-based monitoring system for electric distribution grids," *IEEE Trans. Instrum. Meas.*, vol. 68, no. 10, pp. 3871–3882, Oct. 2019.

[22] R. Abu-Hashim, R. Burch, G. Chang, M. Grady, E. Gunther, M. Halpin, C. Harziadonin, Y. Liu, M. Marz, T. Ortmeyer, V. Rajagopalan, S. Ranade, P. Ribeiro, T. Sim, and W. Xu, "Test systems for harmonics modeling and simulation," *IEEE Trans. Power Del.*, vol. 14, no. 2, pp. 579–587, Apr. 1999.

[23] P. C. Hansen, "REGULARIZATION TOOLS: A Matlab package for analysis and solution of discrete ill-posed problems," *Numerical Algorithms*, vol. 6, no. 1, pp. 1–35, Mar. 1994.

[24] P. C. Hansen, "The discrete picard condition for discrete ill-posed problems," *BIT Numerical Mathematics*, vol. 30, pp. 658–672, 1990.

[25] P. C. Hansen, "The L-curve and its use in the numerical treatment of inverse problems," *P. Johnston (Ed.), Computational Inverse Problems in Electrocar-diography, WIT Press, Southampton*, pp. 119–142, 2001.

[26] V. A. Morozov, *Methods for Solving Incorrectly Posed Problems*. New York, NY: Springer New York, 1984.

[27] D. Carta, C. Muscas, P. A. Pegoraro, A. V. Solinas, and S. Sulis, "Compressive sensing-based harmonic sources identification in smart grids," *IEEE Trans. Instrum. Meas.*, vol. 70, pp. 1–10, 2021.

[28] L. Reichel and A. Shyshkov, "A new zero-finder for Tikhonov regularization," *BIT Numerical Mathematics*, vol. 48, no. 3, pp. 627–643, Sep. 2008.

Carlo Sitzia (S'22) received the M.S. degree (cum laude) in Electrical Engineering in 2020 from the University of Cagliari, Cagliari, Italy, where is currently pursuing the Ph.D. degree with the Electrical and Electronic Measurements Group, Department of Electrical and Electronic Engineering.

His research activity focuses on parameter estimation for modern power networks, phasor measurements and instrument transformers.

Carlo Muscas (M'98, SM'15) received the M.S. degree (cum laude) in electrical engineering from the University of Cagliari, Cagliari, Italy, in 1994. He was an Assistant Professor and an Associate Professor with the University of Cagliari from 1996 to 2001 and from 2001 to 2017, respectively, where he has been a Full Professor of electrical and electronic measurement since 2017.

He has authored and coauthored more than 170 scientific articles. His current research interests include the measurement of synchronized phasors, the implementation of distributed measurement systems for a modern electric grid, and the study of power quality phenomena.

Prof. Muscas is currently the Chairman of the TC 39 Measurements in Power Systems of the IEEE Instrumentation and Measurement Society.

Paolo Attilio Pegoraro (Senior Member, IEEE) received the M.S. (summa cum laude) degree in telecommunication engineering and the Ph.D. degree in electronic and telecommunication engineering from the University of Padova, Padua, Italy, in 2001 and 2005, respectively.

From 2015 to 2018 he was an Assistant Professor with the Department of Electrical and Electronic Engineering, University of Cagliari, Cagliari, Italy, where he is currently Associate Professor. He has authored or co-authored over 120 scientific papers. His current research interests include the development of new measurement techniques for modern power networks, with attention to synchronized measurements and state estimation.

Dr. Pegoraro is a member of TC 39 (Measurements in Power Systems) and of IEC TC 38/WG 47. He is an Associate Editor of the IEEE Transactions on Instrumentation and Measurement.

Antonio Vincenzo Solinas (S'20) received the M.S. degree in Electronic Engineering from University of Cagliari, Italy, in 2000.

Since then, he worked as an R&D manager on audio and video acquisition, compression and transmission over IP.

He is currently a Ph.D. student in the Electrical and Electronic Measurements Group with the Department of Electrical and Electronic Engineering at the University of Cagliari. His main research interests include the optimization techniques for estimation and monitoring in power systems.

Sara Sulis (M'06-SM'19) received the M.S. degree in electrical engineering and the Ph.D. degree in industrial engineering from the University of Cagliari, Cagliari, Italy, in 2002 and 2006, respectively. She is currently an Associate Professor of electrical and electronic measurements with the University of Cagliari.

She has authored or co-authored more than 100 scientific articles. Her current research interests include distributed measurement systems designed to perform state estimation and harmonic sources estimation of distribution networks.

Dr. Sulis is a member of the Instrumentation and Measurement Society, the IEEE TC 39 "Measurements in Power Systems," and the CENELEC TC 38 "Instrument Transformers." She is an Associate Editor of the IEEE Transactions on Instrumentation and Measurement.